

On the Mechanism of Phenol Alkylation in Zeolite H-BEA Using In Situ Solid-State NMR Spectroscopy

Zhenchao Zhao, Hui Shi, Chuan Wan, Mary Y. Hu, Yuanshuai Liu, Donghai Mei, Donald M. Camaioni, Jian Zhi Hu, and Johannes A. Lercher

J. Am. Chem. Soc., **Just Accepted Manuscript** • Publication Date (Web): 19 Jun 2017

Downloaded from <http://pubs.acs.org> on June 19, 2017

Just Accepted

“Just Accepted” manuscripts have been peer-reviewed and accepted for publication. They are posted online prior to technical editing, formatting for publication and author proofing. The American Chemical Society provides “Just Accepted” as a free service to the research community to expedite the dissemination of scientific material as soon as possible after acceptance. “Just Accepted” manuscripts appear in full in PDF format accompanied by an HTML abstract. “Just Accepted” manuscripts have been fully peer reviewed, but should not be considered the official version of record. They are accessible to all readers and citable by the Digital Object Identifier (DOI®). “Just Accepted” is an optional service offered to authors. Therefore, the “Just Accepted” Web site may not include all articles that will be published in the journal. After a manuscript is technically edited and formatted, it will be removed from the “Just Accepted” Web site and published as an ASAP article. Note that technical editing may introduce minor changes to the manuscript text and/or graphics which could affect content, and all legal disclaimers and ethical guidelines that apply to the journal pertain. ACS cannot be held responsible for errors or consequences arising from the use of information contained in these “Just Accepted” manuscripts.



On the Mechanism of Phenol Alkylation in Zeolite H-BEA Using In Situ Solid-State NMR Spectroscopy

Zhenchao Zhao,^{†,1} Hui Shi,^{†,1} Chuan Wan,[†] Mary Y. Hu,[†] Yuanshuai Liu,[‡] Donghai Mei,[†] Donald M. Camaioni,[†] Jian Zhi Hu,^{†,*} Johannes A. Lercher^{†,‡,*}

[†] Institute for Integrated Catalysis, Pacific Northwest National Laboratory, P.O. Box 999, Richland, WA 99352 (United States)

[‡] Department of Chemistry and Catalysis Research Center, TU München, Lichtenbergstrasse 4, 85748 Garching (Germany)

KEYWORDS: *in situ NMR spectroscopy, reaction mechanism, alkylation, zeolites*

ABSTRACT: The reaction mechanism of solid-acid-catalyzed phenol alkylation with cyclohexanol and cyclohexene in the apolar solvent decalin has been studied using in situ ¹³C MAS NMR spectroscopy. Phenol alkylation with cyclohexanol sets in only after a majority of cyclohexanol is dehydrated to cyclohexene. As phenol and cyclohexanol show similar adsorption strength, this strict reaction sequence is not caused by the limited access of phenol to cyclohexanol, but is due to the absence of a reactive electrophile as long as a significant fraction of cyclohexanol is present. ¹³C isotope labeling demonstrates that the reactive electrophile, the cyclohexyl carbenium ion, is directly formed in a protonation step when cyclohexene is the co-reactant. In the presence of cyclohexanol, its protonated dimers at Brønsted acid sites hinder the adsorption of cyclohexene and the formation of a carbenium ion. Thus, it is demonstrated that protonated cyclohexanol dimers dehydrate without the formation of a carbenium ion, which would otherwise have contributed to the alkylation in the kinetically relevant step. Isotope scrambling shows that intramolecular rearrangement of cyclohexyl phenyl ether does not significantly contribute to alkylation at the aromatic ring.

INTRODUCTION

The catalytic conversion of lignin-derived phenolic compounds is a critical pathway for maximizing the utilization of lignocellulosic biomass.¹⁻³ While hydrodeoxygenation increases the H/C ratio and decreases the O/C ratio in the products, (hydro)alkylation adjusts the carbon number and improves the carbon retention in the liquid products.⁴⁻¹⁰ Moreover, alkylated phenols have been widely used as additives in gasoline, lubricants, and consumer products.¹¹⁻¹⁵

Alkylation of phenols, such as phenol or m-cresol, is an electrophilic aromatic substitution. Both olefins and alcohols can be alkylating agents. In the case of alkylation of phenol with olefins, the electrophile is the carbenium ion formed via protonation of the olefin by a Brønsted acid site (BAS) of a solid acid, while in the case of alkylating phenol with alcohol, it is generally a consensus that the electrophile can be the protonated alcohol (an alkoxonium species) or a carbenium ion derived from alcohol dehydration. Electrophilic attack on the phenolic OH or π electrons in the aromatic ring yields O-alkylation or ring-alkylation (C-alkylation) products, respectively. It has also been suggested that C-alkylation products could be formed through intramolecular rearrangement of the kinetically favored O-alkylation product, i.e., via an aryl alkyl ether intermediate product.¹⁶⁻¹⁸

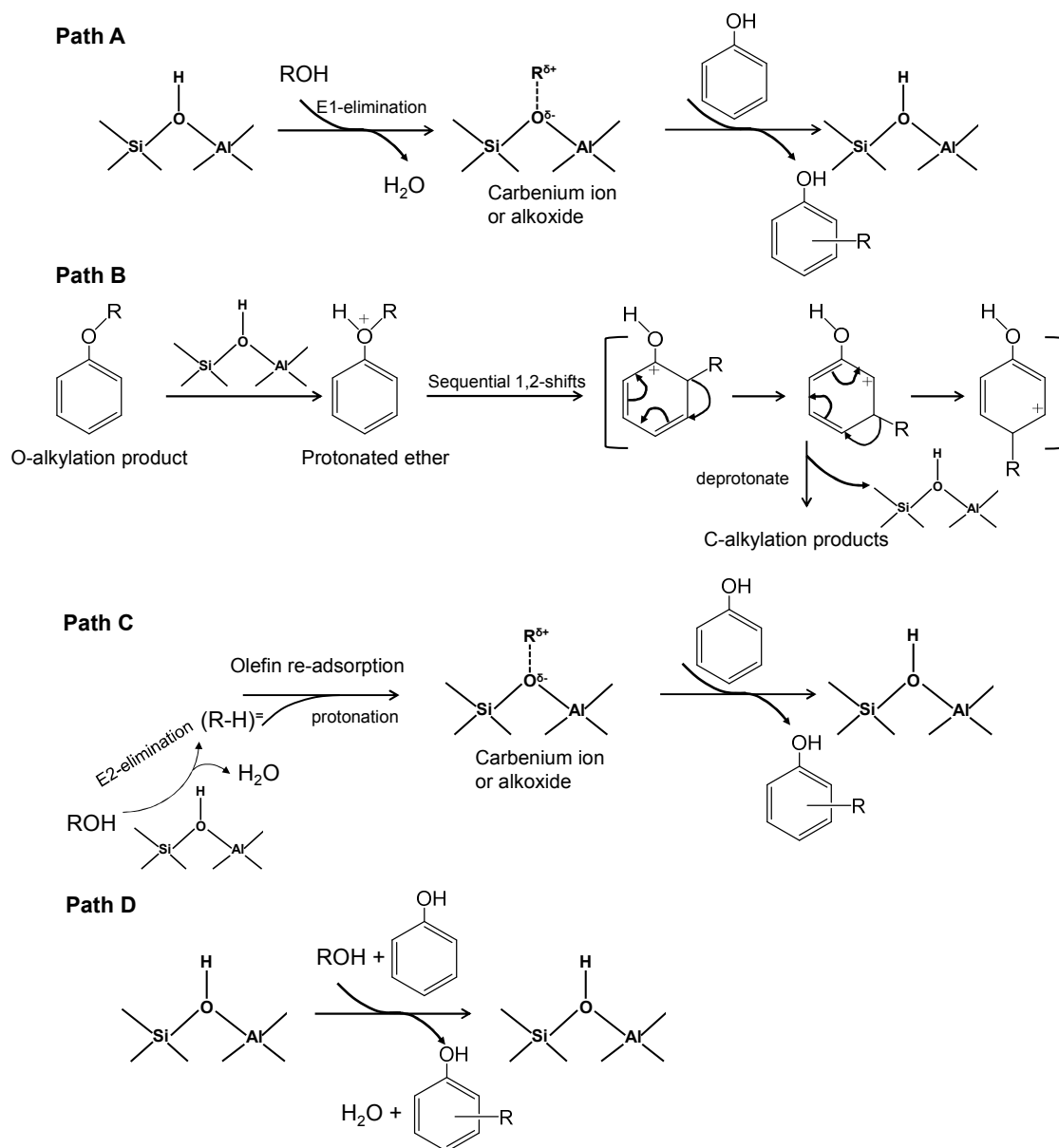
Alkylation of phenols with olefins and alcohols has been extensively studied, in vapor and liquid phases, over a wide range of solid catalysts.^{12-14,19-28} The hypothesized mechanisms from these experimental studies were, however, seldom based on rigorous rate measurements and direct spectroscopic evidence, but rather, almost always “borrowed”/adapted from the

classical Friedel-Crafts alkylation chemistry in a homogeneous phase, or inferred from insufficient and less informative ex situ analyses of reaction products. In particular, for Brønsted acidic zeolites, the mechanism for phenol alkylation with alcohol (e.g., methanol, tert-butyl alcohol) is significantly more controversial, compared to phenol alkylation with olefin (e.g., propene, 1-octene). For example, the contribution of alkyl phenyl ether rearrangement to C-alkylation has been controversially discussed. While some studies reported that an alkyl aryl ether (the kinetically favored product) can undergo facile intramolecular rearrangement to directly produce alkylphenols,^{17,18,27} others negated this pathway, concluding instead that C-alkylation products arise from alkylation of phenol with olefin formed via decomposition of the O-alkylation product.²⁴ From a theoretical point of view, the prevalent mechanism has also remained elusive. Much like the proposals for alkylation of benzene and toluene with methanol,^{29,30} stepwise (i.e., formation of carbenium ion or a covalent surface alkoxide from alcohol, followed by electrophilic substitution) and concerted (i.e., co-adsorption of phenol and alcohol on acid sites and direct conversion in one single elementary step, without the formation of alkoxide or carbenium ion) routes have been proposed for phenol alkylation in zeolites and examined by quantum chemical calculations.^{31,32} Both phenol-methanol alkylation on faujasite zeolite (H-FAU) and tert-butylation of phenol on Beta zeolite (H-BEA) preferentially proceed via a direct, concerted mechanism, rather than via a stepwise mechanism mediated by surface methoxide³¹ or tert-butyl carbenium ion.³² Thus, these theoretical studies appear to challenge the conventional view, at least for the alcohols and zeolites investigated, that carbenium-ion-type

intermediate is involved as the direct electrophile in the major alkylation pathways. However, we note that none of these predictions have been experimentally verified so far for zeolite-catalyzed phenol alkylation. Of particular note is the largely missing application of in situ spectroscopies able to unravel mechanistic pathways for this class of reactions in zeolite pores or on solid surfaces in general.³⁰

We use in situ ¹³C solid-state NMR spectroscopy to probe, at a molecular level, reaction pathways for this type of solid-acid-catalyzed reaction, specifically, alkylation of phenol with cyclohexanol on a large-pore zeolite H-BEA,³³⁻³⁸ using a microautoclave MAS NMR rotor developed for studying multi-phase processes at high temperature, high pressure conditions.^{39,40} The present study was carried out in decalin, a non-polar solvent, which is typical for the environment in which such a reaction would be practically performed.^{24,41} We demonstrate, via analysis of the ¹³C label distribution in olefin

and alkylates, that the carbenium ion (electrophile) is, in fact, not produced directly from the adsorbed cyclohexanol (Scheme 1, path A) in the pore of a BEA zeolite, because the dominant surface species is an alcohol dimer that does not dehydrate via an E1 mechanism. It is also established that intramolecular rearrangement of cyclohexyl phenyl ether is, at best, a minor pathway to cyclohexylphenols (Scheme 1, path B), and that alkylation occurs via a stepwise route initiated by olefin protonation (Scheme 1, path C), instead of a concerted one (Scheme 1, path D). Olefin (re-)adsorption and protonation is the dominant pathway of generating the electrophile for phenol alkylation, regardless of the starting alkylating co-reactant (cyclohexanol or cyclohexene). To the best of our knowledge, this work represents the first example of using NMR to study this class of reactions under steady-state and realistic conditions.³⁰



Scheme 1. Postulated mechanisms for C-alkylation of phenol with alcohol (ROH) on zeolitic protons. (R-H)⁺ stands for olefin.

RESULTS AND DISCUSSION

Variable temperature ^{13}C MAS NMR measurements of phenol and cyclohexanol adsorption on H-BEA from decalin solutions. Figure 1 shows the ^{13}C MAS NMR spectra acquired after reaching adsorption equilibria of $1\text{-}^{13}\text{C}$ -phenol and $1\text{-}^{13}\text{C}$ -cyclohexanol, from their respective decalin solutions, on H-BEA at different temperatures. ^{13}C -isotope scrambling within each molecule was not detected at these temperatures. In each spectrum, a relatively sharp peak representing the mobile species in decalin and a broad peak representing the species adsorbed in H-BEA pores are observed. Specifically, the $1\text{-}^{13}\text{C}$ of phenol in decalin solution appeared at 156.3 ppm, while the $1\text{-}^{13}\text{C}$ of cyclohexanol in decalin was at 69.8 ppm. The corresponding adsorbed species for cyclohexanol was at ~ 71.6 ppm, downfield relative to the mobile species. The adsorbed species for phenol at ~ 155.5 ppm, upfield relative to the solution species. Thus, the $1\text{-}^{13}\text{C}$ signals of cyclohexanol and phenol appear more de-shielded and shielded, respectively, relative to their liquid phase states in decalin. First-principle calculations of NMR chemical shifts for solvation structures of phenol and cyclohexanol in decalin (structures shown in Figure S1) and in the pore of zeolite H-BEA (Figure S2) are qualitatively consistent (Table S2) with the experimental observations.

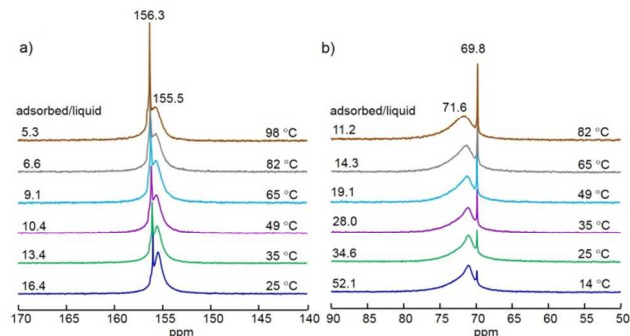


Figure 1. Variable temperature ^{13}C MAS NMR spectra of $1\text{-}^{13}\text{C}$ -phenol (a) and $1\text{-}^{13}\text{C}$ -cyclohexanol (b) adsorption on a H-BEA catalyst (Si/Al = 75).

The peak area ratio of adsorbed and mobile phase phenol decreased from 16.4 to 6.6, while that ratio for cyclohexanol decreased from 34.6 to 11.2, with increasing adsorption temperature. This indicates that the uptake from decalin into H-BEA pores is exothermic for both molecules. The solution concentrations at adsorption equilibria (C_{eq}) and uptakes (q) for phenol and cyclohexanol at different adsorption temperatures are compiled in Table S3, Supporting Information. The uptake values ($1.0\text{--}1.3\text{ mmol g}_{\text{H-BEA}}^{-1}$) were all much higher than a 1:1 coverage of BAS ($\sim 0.15\text{ mmol g}_{\text{H-BEA}}^{-1}$), indicating that most of the adsorbed species were present physisorbed in the pores without directly interacting with the BAS. The molar ratios of adsorbed and solution species are comparable for cyclohexanol and phenol at any given temperature, suggesting that the adsorption constant and enthalpy of adsorption in H-BEA pores were very similar for the two molecules. Consistent with these in situ measurements, independent ex-situ measurements for the same mixtures provided

adsorption constants of 44 and 73 (at 25 °C) for phenol and cyclohexanol, respectively (data not shown).

Alkylation of $1\text{-}^{13}\text{C}$ -phenol with $1\text{-}^{13}\text{C}$ -cyclohexanol. During the first ~ 400 min, cyclohexanol dehydration was almost the only reaction taking place (Figure 2). $1\text{-}^{13}\text{C}$ -cyclohexanol (70.2 ppm) dehydration led to $1\text{-}^{13}\text{C}$ -cyclohexene (127.2 ppm) as the primary product, while the $3\text{-}^{13}\text{C}$ and $4\text{-}^{13}\text{C}$ isotopomers of cyclohexene increased in concentration at longer residence times. A weak signal of dicyclohexyl ether at 74.8 ppm disappeared quickly (Figure S3, Supporting Information). The rate of phenol alkylation started to increase ($\sim 4 \times 10^{-5}\text{ mol g}_{\text{H-BEA}}^{-1}\text{ min}^{-1}$ at 127 °C) only after most cyclohexanol was dehydrated. For mono-alkylation, the ortho to para substitution occurred initially in a 1:1 ratio, but gradually increased to values larger than 1. This ratio was still lower than the statistical ratio (2:1), indicating that the pore constraints of H-BEA influence the product selectivity (see also Table S4, Supporting Information). Meta-substitution was not detected. Di-alkylation occurred much later, producing only 2,4-dicyclohexyl phenol.

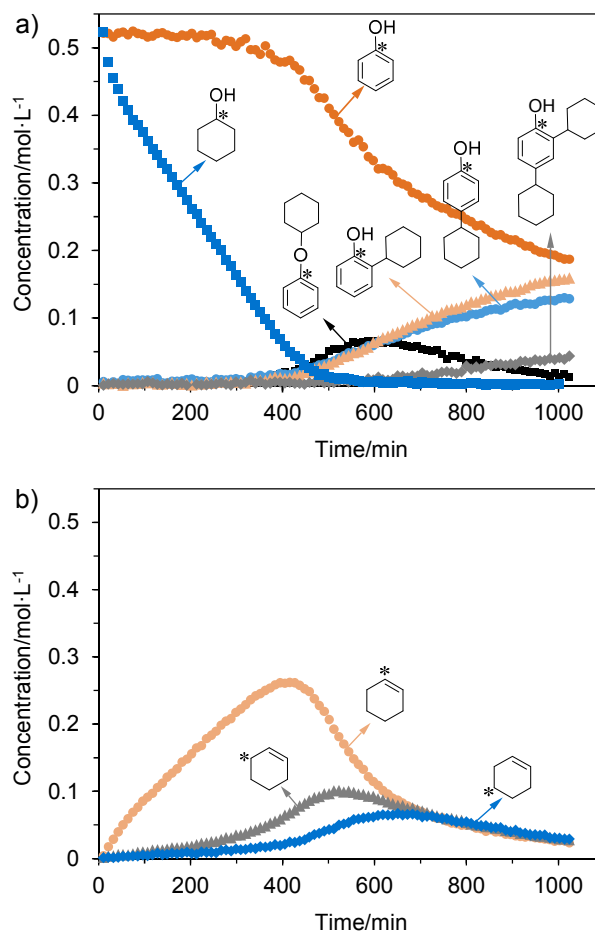


Figure 2. Concentration-time profiles of (a) reactants and alkylation products as well as (b) dehydration products during the in situ NMR investigation of phenol-cyclohexanol reaction catalyzed by H-BEA at 127 °C.

The series of in situ ^{13}C MAS NMR spectra in the aromatic carbon region (Figure 3) as a function of reaction time shows that the signal at 156.5 ppm representing $1\text{-}^{13}\text{C}$ -phenol started to decrease after 400 min, with the appearance of cyclohexyl phenyl ether, 4-cyclohexylphenol, 2-cyclohexylphenol, and 2,4-dicyclohexyl phenol at 158.8, 154.5, 153.6, and 151.6 ppm (all at 1-C position for phenol), respectively, without label scrambling in phenol.

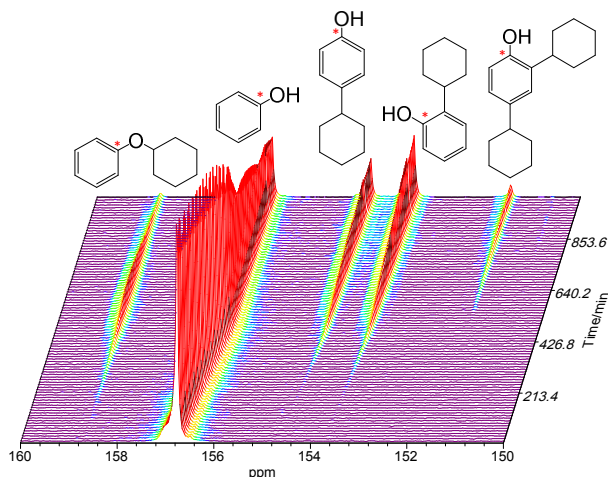


Figure 3. Stacked plot of in situ ^{13}C MAS NMR spectra (aromatic carbon region) of $1\text{-}^{13}\text{C}$ -phenol alkylation with $1\text{-}^{13}\text{C}$ -cyclohexanol at $127\text{ }^\circ\text{C}$. The initial concentrations of phenol and cyclohexanol were 0.54 and 0.51 M (based on density of solution at room temperature), respectively. For other carbon regions, see Figure S3.

While the concentration of cyclohexyl phenyl ether (peak at 158.8 ppm) gradually decreased after reaching the maximum concentration at 600 min, the C-alkylation products continued to increase with increasing residence time (see Figure S4 for ^{13}C signals at chemical shifts of 20–45 ppm related to the carbons on the cyclohexyl ring). This shows that ethers formed by the kinetically faster O-alkylation are converted further, while the ring alkylation products (C-alkylation) are stable end products.

The fact that phenol alkylation did not start until cyclohexanol was almost completely consumed suggests that either phenol, or the direct alkylating agent (electrophile), or both, are significantly weaker in interacting with acid sites than cyclohexanol (or its derived surface intermediate). As phenol and cyclohexanol have similar adsorption constants in the zeolite pores, the lack of phenol alkylation before most cyclohexanol was dehydrated (Figure 2) is concluded not to result from the absence of phenol at the BAS. Instead, we hypothesize that only cyclohexene forms the reactive intermediate (while cyclohexanol does not) for ring alkylation and that the adsorption constant for cyclohexene at the BAS is too low for it to compete with cyclohexanol at appreciable concentrations of the latter. Alcohol molecules are known to form protonated dimers⁴²⁻⁴⁴ at BAS, which are dominant surface species even at low concentrations or partial pressures.^{42,43} Such adsorbed species (i.e., alcohol dimer, phenol-alcohol adsorption complex) in H-BEA pores, however, were not directly observed by NMR spectroscopy

under the present alkylation conditions (i.e., higher temperature and an 18-time larger substrate-to-catalyst ratio than used in adsorption experiments; see Experimental).

Alkylation of $1\text{-}^{13}\text{C}$ -phenol with cyclohexene. When cyclohexene (unlabeled) was used to alkylate phenol, the concentration of phenol decreased exponentially with the reaction time (Figures 4, S5 and S6). Both O- and C-alkylation were observed from the beginning of the reaction. Similar to the case of phenol alkylation with cyclohexanol, cyclohexyl phenyl ether quickly reached the maximum and then disappeared, whereas all C-alkylation products continued to grow until cyclohexene was fully consumed after 250 min. The formation of cyclohexyl phenyl ether was kinetically favored and reversible. The reversibility of O-alkylation is also shown by the rapid formation of cyclohexene, phenol and alkylation products when cyclohexyl phenyl ether was used as reactant (Figure S7). 2,4-Dicyclohexyl phenol, the only di-alkylation product observed, increased more rapidly than in phenol-cyclohexanol alkylation. The final ratio of ortho- and para-monoalkylation was ~ 1.5 , similar to that obtained in phenol-cyclohexanol alkylation and lower than the statistical ratio of 2:1.

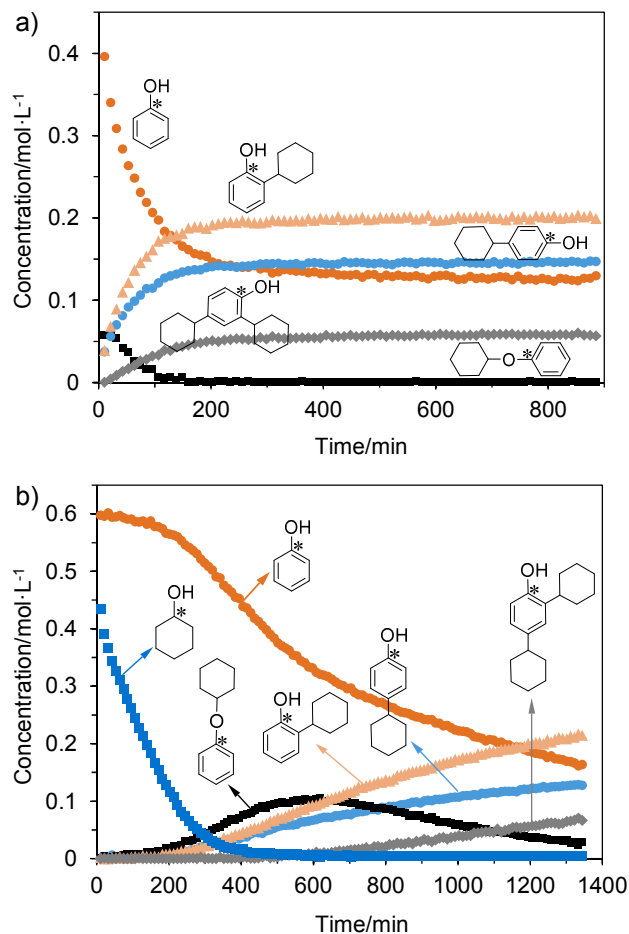


Figure 4. Concentration-time profile of compounds during the in situ NMR investigation of H-BEA-catalyzed alkylation of phenol with cyclohexene (un-labeled) only (a) and with equimolar cyclohexene and $1\text{-}^{13}\text{C}$ -cyclohexanol (b) at $127\text{ }^\circ\text{C}$.

With cyclohexanol initially added together with cyclohexene, all alkylation reactions were drastically retarded and became faster only after a major fraction of cyclohexanol was dehydrated (Figure 4). This, combined with the initial lack of alkylation for the phenol-cyclohexanol-decalin mixture (0-400 min in Figure 2a), allows us to conclude that: (a) the electrophile for alkylating phenol is not formed in the reaction path of cyclohexanol dehydration; (b) the presence of cyclohexanol inhibits the formation of the electrophile from the olefin. Note that the concentration of phenol hardly changed in the zeolite pores as alcohol dehydration progressed.

Nature of the alkylating agent. Figure 5 shows the ^{13}C signal intensities for all the products (dehydration product: cyclohexene; alkylation products: cyclohexyl phenols and cyclohexyl phenyl ether) present in the reaction mixture of 1- ^{13}C -phenol alkylation with 1- ^{13}C -cyclohexanol. During alkylation, the ^{13}C label in phenol did not undergo scrambling, while a small extent of label scrambling was observed for cyclohexanol (Figures S4 and S8).

As mentioned before, the 3- ^{13}C and 4- ^{13}C isotopomers of cyclohexene were essentially secondary products (Figures 2b and S9). Two possible reaction paths for the observed ^{13}C scrambling in cyclohexene during 1- ^{13}C -cyclohexanol dehydration exist: (1) ^{13}C scrambling via hydride shifts in an intermediately formed carbenium ion via E1-type elimination of water from a protonated cyclohexanol, and (2) cyclohexene re-adsorption and protonation at the BAS, forming cyclohexyl carbenium ion with the ^{13}C label at either the 1- or 2-position, which may also scramble the labels by hydride shift. If ^{13}C scrambling occurs by hydride shift of the 1- ^{13}C -cyclohexyl carbocation directly formed from E1-type elimination, then rapid hydride shifts of this carbenium ion would form 2-, 3-, and 4- ^{13}C -cyclohexyl carbocations and subsequent deprotonation steps would lead to 3- and 4- ^{13}C -cyclohexene accompanying 1- ^{13}C -cyclohexene even at the initial stage. This is indeed the case for aqueous phase dehydration of cyclohexanol on the same H-BEA catalyst.⁴⁰ However, as illustrated in Figure 2b and Figure 5a, there was little formation of 3- or 4- ^{13}C -cyclohexene during the initial 200 min. The negligible scrambling at the initial stage indicates that the dominant surface species at this concentration, the protonated cyclohexanol dimer,⁴²⁻⁴⁴ does not form a carbenium ion during dehydration. As the ^{13}C scrambling rate increased significantly only after 500 min, when most cyclohexanol was consumed, it is concluded that ^{13}C scrambling in cyclohexene occurs via re-adsorption and protonation of cyclohexene. We conclude also that re-adsorption of cyclohexene is significantly hindered by the presence of cyclohexanol, but not by phenol. The ^{13}C labels in olefin products were fully randomized after ~700 min (Figure 5a), suggesting rapid protonation-deprotonation equilibrium for the olefin.

Figure 5b shows the integrated ^{13}C signal intensities for ortho- and para-substituted 1- and 2- ^{13}C -cyclohexylphenols as a function of reaction time. The 3- and 4- ^{13}C -labeled isotopomers of o- and p-cyclohexylphenols were also detected in significant concentrations (26-28 ppm, Figure S4), but were not included in Figure 5b because of the difficulty in completely separating their signals from natural abundance ^{13}C

signals associated with the solvent, decalin. Moreover, the chemical shifts for ^{13}C -labels at 3- and 4-positions in the cyclohexyl ring significantly overlap with each other (Table S1), and thus, the two could not be unequivocally differentiated from each other. In an attempt to subtract the solvent peak, it was found that the sum of the integrated intensities for 3- and 4- ^{13}C -cyclohexylphenols (non-solvent peaks in the 26-28 ppm range) was approximately 1.4 times that for the 2- ^{13}C -cyclohexylphenols (in the range of 33-36 ppm) after complete scrambling of ^{13}C labels in the olefin.

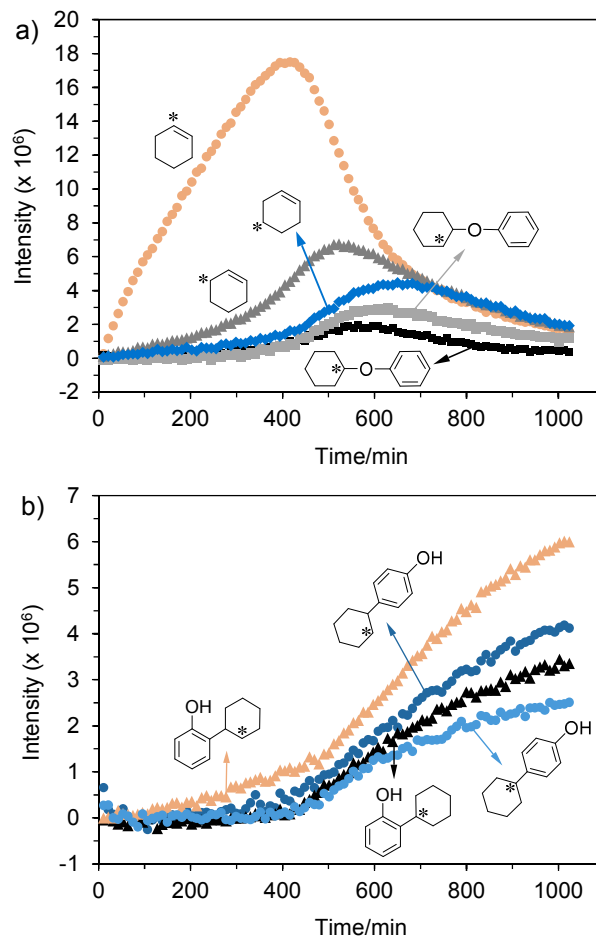


Figure 5. Integrated ^{13}C signal intensities of (a) dehydration and (b) ortho- and para-alkylation products during phenol alkylation with 1- ^{13}C -cyclohexanol on H-BEA in decalin (unlabeled) as a function of reaction time at 127 °C. The relatively large scatters in (b) at the beginning originate from the subtraction of the intensities of decalin-related peaks (which overlap with some of the naphthenic carbon signals in cyclohexyl) from the total signal intensities.

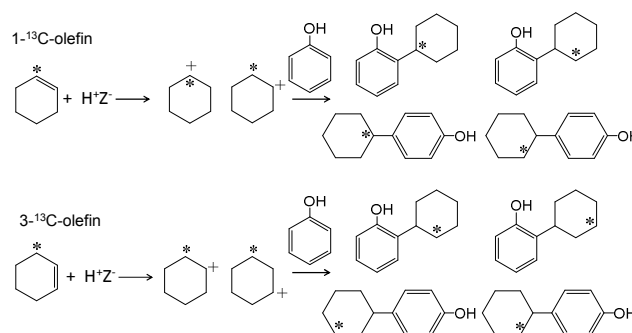
For both o- and p-monoalkylation, the concentrations of 2- ^{13}C -cyclohexyl phenols were generally higher than 1- ^{13}C -cyclohexyl phenols. This became evident at $t > 200$ min, and by the end of the experiment, 2- ^{13}C -cyclohexyl phenols had reached concentrations nearly twice (~ 1.8-fold) those of the 1- ^{13}C -cyclohexyl counterparts. If phenol reacted with the intermediate directly generated from dehydration of 1- ^{13}C -

cyclohexanol, before significant hydride shift had occurred, most of the C-alkylation products would have contained 1-¹³C-cyclohexyl. Even if rapid hydride shifts had occurred, the transient concentration of the 2-¹³C-cyclohexyl carbocation, or any other secondary carbocation intermediate (e.g., 3- and 4-¹³C-cyclohexyl carbocations), at any given time should always be lower than, or at most equal to (fully equilibrated hydride shifts, see Figure S10), that of the 1-¹³C-cyclohexyl carbocation (a primary kinetic intermediate from E1-elimination). Consequently, alkylation of phenol by intermediates directly produced from cyclohexanol dehydration is not able to account for the observed preference for 2-¹³C-cyclohexyl phenols (Figure 5b). The results are fully consistent, however, with re-adsorption and protonation of cyclohexene at the BAS that forms more 2-¹³C-cyclohexyl carbenium ion than 1-¹³C-cyclohexyl carbenium ion at all reaction times. A concerted mechanism, with co-adsorbed phenol and alcohol reacting in a single step to form alkylates,³⁰⁻³² can also be excluded, because it would require that the C- and O-alkylates should contain ¹³C labels at the same position as in the alcohol, i.e., 1-¹³C-cyclohexanol in this case. Note that the concerted mechanism is also inconsistent with the negligible alkylation as long as cyclohexanol is present (Figure 2a).

Finally, if a major part of the C-alkylation were formed via intramolecular rearrangement of cyclohexyl phenyl ether (Scheme 1, path B), the ¹³C position of the cyclohexyl group should not change during cyclohexyl group migration according to the alkyl group migration mechanism.¹⁷ Figure 5a shows that the concentration of 1-¹³C-cyclohexyl phenol ether was similar to 2-¹³C-cyclohexylphenol ether for the first 400 min and became slightly lower than 2-¹³C-cyclohexylphenol ether afterwards. Since 2-¹³C-cyclohexyl phenols remained to be significantly higher in concentration than 1-¹³C-cyclohexyl phenols, intramolecular rearrangement of O-alkylation products is excluded to be a major pathway for C-alkylation.

Thus, phenol alkylation with cyclohexanol occurs via a step-wise mechanism, where the carbenium ion from olefin protonation is the main alkylating agent (Scheme 1, path C). 1-¹³C-cyclohexyl carbenium ion is only produced from re-adsorption and protonation of 1-¹³C-cyclohexene, whereas 2-¹³C-cyclohexyl carbenium ion can be produced from re-adsorption and protonation of both 1- and 3-¹³C-cyclohexenes, as shown in Scheme 2. The lack of alkylation, until most cyclohexanol was dehydrated (0–400 min in Figure 2a), is concluded to be a consequence of the acid sites interacting with cyclohexanol dimers, which eliminate water via a pathway not involving carbenium ion-type intermediate (by inference, an E2-pathway). The rate acceleration of alkylation at $t > 400$ min is, therefore, attributed to the increased concentration of carbenium ions produced from olefin re-adsorption and protonation at the BAS, once the alcohol-derived species are significantly depleted by dehydration. After the labels in olefins were fully randomized, the estimated ratio between 1-¹³C, 2-¹³C and (3+4)-¹³C labeled cyclohexylphenols was 1.0: 1.8(±0.1): 2.6(±0.2). This ratio was independent of the temperature (119–142 °C) and reasonably close to the theoretical ratio (1: 2: (2+1)) for the C-alkylation products that are proposed to form via quasi-equilibrated olefin protonation followed by electrophilic attack (Figure S10). Rapid scrambling of the labels within the carbenium ion (e.g., via hydride shifts or multiple deprotonation-protonation events), compared to the electro-

philic attack step, would lead to equal distribution of labels among all positions for a given monoalkylation product, not in line with the observations. Taken together, we conclude that phenol must be in the vicinity of the acid site and the carbenium ion so that the carbenium ion is trapped before extensive label shifts can occur.



Scheme 2. Re-adsorption and protonation of cyclohexene at the BAS leads to o- and p-substituted C-alkylation products (O-alkylation and di-alkylation products not shown) that contain more 2-¹³C-cyclohexyl (upper and lower paths) than 1-¹³C-cyclohexyl (upper path only). H⁺Z stands for a BAS of zeolite. Hydride shift pathways are not shown.

CONCLUSION

Phenol alkylation with cyclohexanol in decalin occurs primarily via electrophilic attack of a cyclohexyl cation, not an alkoxonium ion, on the phenolic OH or π electrons in the aromatic ring. As cyclohexanol needs to be almost completely dehydrated before the rate of alkylation is measurable, the dehydration of cyclohexanol is concluded not to involve a surface intermediate able to alkylate the aromatic ring of phenol. Intramolecular rearrangement of the kinetically favored, reversibly formed cyclohexyl phenyl ether is also not a significant pathway leading to C-alkylation products. At the initial stage of phenol-cyclohexanol alkylation, the presence of cyclohexanol hinders the adsorption of cyclohexene at the Brønsted acid site and the subsequent formation of the carbenium ion. The latter is generated upon re-adsorption and protonation of cyclohexene, with increasing propensity with decreasing alcohol concentrations. The carbenium ion is only generated via protonation of cyclohexene. Thus, with cyclohexene used as alkylating agent, higher rates of alkylation were observed than when cyclohexanol was the co-reactant. The ¹³C label distribution in the alkylation products indicates that the carbenium ion generated from olefin protonation is rapidly trapped by phenol before extensive label scrambling occurs. The observations in this work imply that for industrial realization, as well as for synthetic purposes, the use of two catalyst beds, one for dehydration and a second for alkylation, may allow the optimization of an overall alkylation process.

EXPERIMENTAL SECTION

The H-BEA (Si/Al = 75) sample was provided by Clariant and was used and characterized previously.^{40,45} The choice of this material allowed us to attribute the measured activity exclusively to Brønsted acid sites, as it contains very low concentra-

tions of Lewis-acidic extraframework Al species.⁴⁵ All chemicals were purchased from Sigma-Aldrich and used as received. Adsorption measurements and catalytic reactions of 1-¹³C-cyclohexanol (99 atom % ¹³C-enriched) and 1-¹³C-phenol (99 atom % ¹³C-enriched) on H-BEA were conducted in a home-made high temperature high pressure MAS NMR rotor, where decalin (> 99%, anhydrous mixture of cis + trans) was used as the solvent. Other chemicals included cyclohexene (≥ 99%) and cyclohexyl phenyl ether (95%).

Typically, for variable temperature (VT) adsorption experiments, 10 mg 1-¹³C-cyclohexanol or 10 mg 1-¹³C-phenol mixed with 177 mg decalin and 82 mg H-BEA were loaded in the rotor. The adsorption temperature was varied from 0 to 115 °C for phenol and from 0 to 82 °C for cyclohexanol, and maintained at each set point for 0.5-1 h until no change could be observed in the ¹³C signals of adsorbed or dissolved phenol/cyclohexanol. The temperature and the amount of zeolite, decalin and reactants loaded in the rotor were somewhat different for the various reaction experiments: 1) cyclohexanol-phenol alkylation: 127 °C, 10.6 mg 1-¹³C-cyclohexanol, 10.1 mg 1-¹³C-phenol, 178 mg decalin and 4.6 mg H-BEA; 2) cyclohexanol dehydration: 126 °C, 9.6 mg 1-¹³C-cyclohexanol, 194 mg decalin and 4.6 mg H-BEA; 3) cyclohexene-phenol alkylation: 128 °C, 8.1 mg cyclohexene (unlabeled), 10.2 mg 1-¹³C-phenol, 182 mg decalin and 4.9 mg H-BEA; 4) cyclohexene-cyclohexanol-phenol alkylation: 128 °C, 9 mg cyclohexene (unlabeled), 9.2 mg 1-¹³C-cyclohexanol, 11.3 mg 1-¹³C-phenol, 178 mg decalin and 5.3 mg H-BEA; 5) cyclohexyl phenyl ether decomposition: 142 °C, 100 mg cyclohexyl phenyl ether (unlabeled), 88 mg decalin and 4.1 mg H-BEA.

In situ ¹³C MAS NMR measurements were carried out on a Varian 500 MHz NMR spectrometer using a 7.5 mm HX MAS probe with a spinning rate of 3.1 kHz at a resonance frequency of 125.7 MHz. The VT experiments were conducted using a commercially available heating stack provided by Varian, and the actual temperature in the rotor was calibrated using ethylene glycol using a protocol reported in the literature.⁴⁶ ¹³C MAS NMR spectra were recorded using a $\pi/2$ pulse with pulse width of 5.5 μ s and ¹H TPPM decoupling during data acquisition. For each spectrum, 64 scans were accumulated with a 10 s recycle delay, which we conclude to be sufficient for quantification purposes based on the equal intensities of signals collected using 10-30 s recycle delays. The carbon balance was better than 96% throughout the reaction, based on the total integrated intensities of signals corresponding to all the compounds (except decalin). The chemical shifts were referenced to adamantane with the upfield methine peak at 29.5 ppm. All the alkylation products were quantified based on the signal of 1-¹³C in the aromatic ring. A table compiling all the chemical shift values of pertinent compounds is presented in the Supporting Information (Table S1).

ASSOCIATED CONTENT

Supporting Information.

Additional figures, tables and details for the theoretical calculations of chemical shifts. This material is available free of charge via the Internet at <http://pubs.acs.org>.

AUTHOR INFORMATION

Corresponding Author

*Jianzhi.Hu@pnnl.gov

*Johannes.Lercher@ch.tum.de, johannes.lercher@pnnl.gov

Author Contributions

¹These authors contributed equally to this work. The manuscript was written through contributions of all authors. All authors have given approval to the final version of the manuscript.

Notes

The authors declare no competing financial interest.

ACKNOWLEDGMENT

The authors would like to thank Prof. Gary L. Haller for his careful reading of the manuscript. This research was supported by the U. S. Department of Energy (DOE), Office of Basic Energy Sciences, Division of Chemical Sciences, Biosciences and Geosciences. All of the NMR experiments were performed in the Environmental Molecular Sciences Laboratory (EMSL), a national scientific user facility sponsored by the DOE's Office of Biological and Environmental Research, and located at Pacific Northwest National Laboratory (PNNL). PNNL is a multi-program national laboratory operated for the DOE by Battelle Memorial Institute under Contract DE-AC06-76RLO 1830.

REFERENCES

- Huber, G. W.; Iborra, S.; Corma, A. *Chem. Rev.* **2006**, 106, 4044.
- Zakzeski, J.; Bruijninx, P. C. A.; Jongerius, A. L.; Weckhuysen, B. M. *Chem. Rev.* **2010**, 110, 3552.
- Besson, M.; Gallezot, P.; Pinel, C. *Chem. Rev.* **2014**, 114, 1827.
- Demirbas, A. *Energ. Convers. Manage.* **2009**, 50, 2782.
- Zhao, C.; Camaioni, D. M.; Lercher, J. A. *J. Catal.* **2012**, 288, 92.
- Zhao, C.; Song, W.; Lercher, J. A. *ACS Catal.* **2012**, 2, 2714.
- Xu, W.; Miller, S. J.; Agrawal, P. K.; Jones, C. W. *Catal. Lett.* **2014**, 144, 434.
- Nie, L.; Resasco, D. E. *Appl. Catal. A* **2012**, 447, 14.
- Xu, W.; Miller, S. J.; Agrawal, P. K.; Jones, C. W. *Appl. Catal. A* **2013**, 459, 114.
- Zhang, Z.; Wang, Q.; Tripathi, P.; Pittman Jr, C. U. *Green Chem.* **2011**, 13, 940.
- Velu, S.; Swamy, C. S. *Appl. Catal. A* **1994**, 119, 241.
- Lee, S. C.; Lee, S. W.; Kim, K. S.; Lee, T. J.; Kim, D. H.; Kim, J. C. *Catal. Today* **1998**, 44, 253.
- Hu, C. W.; Zhang, Y. F.; Xu, L.; Peng, G. *Appl. Catal. A* **1999**, 177, 237.
- Sato, S.; Takahashi, R.; Sodesawa, T.; Matsumoto, K.; Kamimura, Y. *J. Catal.* **1999**, 184, 180.
- Schmidt, R. J. *Appl. Catal. A* **2005**, 280, 89.
- Dewar, M. J. S.; Putnam, N. A. *J. Chem. Soc. (Resumed)* **1959**, 4086.
- Ma, Q. S.; Chakraborty, D.; Faglioni, F.; Muller, R. P.; Goddard, W. A.; Harris, T.; Campbell, C.; Tang, Y. C. *J. Phys. Chem. A* **2006**, 110, 2246.
- Bregolato, M.; Bolis, V.; Busco, C.; Ugliengo, P.; Bordiga, S.; Cavani, F.; Ballarini, N.; Maselli, L.; Passeri, S.; Rossetti, I.; Forni, L. *J. Catal.* **2007**, 245, 285.
- Choi, W. C.; Kim, J. S.; Lee, T. H.; Woo, S. I. *Catal. Today* **2000**, 63, 229.

- 1 (20) DeCastro, C.; Sauvage, E.; Valkenberg, M. H.; Hölderich,
W. F. J. *Catal.* **2000**, 196, 86.
- 2 (21) Hajipour, A. R.; Karimi, H. *Appl. Catal. A* **2014**, 482, 99.
- 3 (22) Anand, R.; Gore, K. U.; Rao, B. S. *Catal. Lett.* **2002**, 81,
33.
- 4 (23) Beltrame, P.; Zuretti, G. *Green Chem.* **2004**, 6, 7.
- 5 (24) González-Borja, M. Á.; Resasco, D. E. *AIChE J.* **2015**, 61,
598.
- 6 (25) Mathew, T.; Vijayaraj, M.; Pai, S.; Tope, B. B.; Hegde, S.
G.; Rao, B. S.; Gopinath, C. S. *J. Catal.* **2004**, 227, 175.
- 7 (26) Ronchin, L.; Vavasori, A.; Toniolo, L. *J. Mol. Catal. A*
2012, 355, 134.
- 8 (27) Ronchin, L.; Quatarone, G.; Vavasori, A. *J. Mol. Catal. A*
2012, 353-354, 192.
- 9 (28) Wang, W.; De Cola, P. L.; Glaeser, R.; Ivanova, I.;
Weitkamp, J.; Hunger, M. *Catal. Lett.* **2004**, 94, 119.
- 10 (29) Vos, A. M.; Nulens, K. H. L.; de Proft, F.; Schoonheydt, R.
A.; Geerlings, P. *J. Phys. Chem. B* **2002**, 106, 2026.
- 11 (30) Svelle, S.; Visur, M.; Olsbye, U.; Saepurahman, S.;
Björgen, M. *Top. Catal.* **2011**, 54, 897.
- 12 (31) Jansang, B.; Nanok, T.; Limtrakul, J. *J. Phys. Chem. C*
2008, 112, 540.
- 13 (32) Nie, X.; Janik, M. J.; Guo, X.; Liu, X.; Song, C. *Catal. To-
day* **2011**, 165, 120.
- 14 (33) Radhakrishnan, S.; Goossens, P.-J.; Magusin, P. C. M. M.;
Sree, S. P.; Detavernier, C.; Breynaert, E.; Martineau, C.; Taulelle, F.;
Martens, J. A. *J. Am. Chem. Soc.* **2016**, 138, 2802.
- 15 (34) Ivanova, I. I.; Kolyagin, Y. G. *Chem. Soc. Rev.* **2010**, 39,
5018.
- 16 (35) Haw, J. F.; Song, W.; Marcus, D. M.; Nicholas, J. B. *Acc.
Chem. Res.* **2003**, 36, 317.
- 17 (36) Haouas, M.; Walspurger, S.; Taulelle, F.; Sommer, J. J.
Am. Chem. Soc. **2004**, 126, 599.
- 18 (37) Wang, W.; Jiang, Y.; Hunger, M. *Catal. Today* **2006**, 113,
102.
- 19 (38) Wang, C.; Wang, Q.; Xu, J.; Qi, G.; Gao, P.; Wang, W.;
Zou, Y.; Feng, N.; Liu, X.; Deng, F. *Angew. Chem. Int. Ed.* **2016**, 55,
2507.
- 20 (39) Hu, J. Z.; Hu, M. Y.; Zhao, Z.; Xu, S.; Vjunov, A.; Shi, H.;
Camaioni, D. M.; Peden, C. H. F.; Lercher, J. A. *Chem. Commun.*
2015, 51, 13458.
- 21 (40) Vjunov, A.; Hu, M. Y.; Feng, J.; Camaioni, D. M.; Mei, D.;
Hu, J. Z.; Zhao, C.; Lercher, J. A. *Angew. Chem. Int. Ed.* **2014**, 53,
479.
- 22 (41) Espeel, P. H. J.; Vercruyssen, K. A.; Debaerdemaker, M.;
Jacobs, P. A. in: *Studies in Surface Science and Catalysis*,
J. Weitkamp, H. G. Karge, H. Pfeifer, W. Hölderich, Eds., vol. 84,
Elsevier, Amsterdam, **1994**, pp. 1457.
- 23 (42) Macht, J.; Janik, M. J.; Neurock, M.; Iglesia, E. *J. Am.
Chem. Soc.* **2008**, 130, 10369.
- 24 (43) Zhi, Y.; Shi, H.; Mu, L.; Liu, Y.; Mei, D.; Camaioni, D.
M.; Lercher, J. A. *J. Am. Chem. Soc.* **2015**, 137, 15781.
- 25 (44) Lee, K. Y.; Arai, T.; Nakata, S.; Asaoka, S.; Okuhara, T.;
Misono, M. *J. Am. Chem. Soc.* **1992**, 114, 2836.
- 26 (45) Vjunov, A.; Fulton, J. L.; Camaioni, D. M.; Hu, J. Z.; Bur-
ton, S. D.; Arslan, I.; Lercher, J. A. *Chem. Mater.* **2015**, 27, 3533-
3545.
- 27 (46) Ammann, C.; Meier, P.; Merbach, A. *J. Magn. Res.* **1982**,
46, 319.

For Table of Contents Only

